American Journal of Environmental Protection, 2022, Vol. 10, No. 1, 8-21
Available online at http://pubs.sciepub.com/env/10/1/2
Published by Science and Education Publishing
DOI:10.12691/env-10-1-2

Spatio-temporal Analysis of Surface and Root Zone Soil Moisture Derived from SMAP and SMOS Microwave Satellite Data Using in-situ Measurements in Senegal

Omar Marigo[1,2,*], Gayane Faye[1], Manuela Grippa[3], Thierry Pellarin[4], Modou Mbaye[1], Dome Tine[1,5], Eric Mougin[3], Fama Mbengue[1,2], Aissata Thiam[1], Balla Diop Ngom[2]

[1]Laboratoire de Télédétection Appliquée (LTA), Institut des Sciences de la Terre (IST), Université Cheikh Anta DIOP (UCAD) of Dakar, Senegal
[2]Department of Physic, Faculty of Science and Technology, Université Cheikh Anta DIOP (UCAD) of Dakar, Senegal
[3]Géosciences Environnement Toulouse (Université de Toulouse III, CNRS, IRD, CNES), France
[4]Université de Grenoble Alpes, CNRS, IRD, Grenoble INP, IGE, Grenoble F-38000, France
[5]Department of Geography, Université Cheikh Anta DIOP (UCAD) of Dakar- Senegal
*Corresponding author: omar.marigo@ucad.edu.sn

Received February 12, 2022; Revised March 15, 2022; Accepted March 23, 2022

Abstract Soil moisture plays a regulating role on Earth-Atmosphere flux and the water balance at the terrestrial surface. In recent years, significant progress has been made in quantifying soil moisture from satellite data. Particularly, microwave space remote sensing remains an efficient tool for estimating soil moisture at a large scale. However, the validation by in situ measurements is still needed in some areas such as the Sahel, especially for elaborated products such as soil moisture in the root zone. The present study is contributing to the validation of soil moisture products in the silvopastoral and agricultural system within the Sahelian area in Senegal. Soil moisture products derived from Soil Moisture Active and Passive (SMAP) sensors at 9 and 36 km and Soil Moisture Ocean Salinity (SMOS) at the resolution of 0.25° x 0.25° are compared with in-situ measurements acquired at different depths (from 0 to 100 cm) three validation sites. First, a validation of the in-situ measurements was done to visualize the performance of these sensors in situ for soil moisture recovery on the three study sites (Loumbi, Bawdi, and Niakhar). Second, an estimation of the SMAP, SMOS products of the surface area (5 cm depth) was made. Third, an estimation showed that these microwave sensors follow the soil moisture dynamics whatever the surface and climatic conditions and also despite RMSE higher or equal to the specifications, 0.04 m^3/m^3. Finally, the results from the soil moisture analysis of the root zone of the satellite and in-situ products are very important.

Keywords: *validation, soil moisture, SMAP, SMOS, microwave remote sensing, Senegal*

Cite This Article: Omar Marigo, Gayane Faye, Manuela Grippa, Thierry Pellarin, Modou Mbaye, Dome Tine, Eric Mougin, Fama Mbengue, Aissata Thiam, and Balla Diop Ngom, "Spatio-temporal Analysis of Surface and Root Zone Soil Moisture Derived from SMAP and SMOS Microwave Satellite Data Using in-situ Measurements in Senegal." *American Journal of Environmental Protection*, vol. 10, no. 1 (2022): 8-21. doi: 10.12691/env-10-1-2.

1. Introduction

Soil moisture (SM) is an essential parameter for characterizing surface conditions relevant to the ecosystem, weather forecasting, climate prediction, agricultural productivity, flooding, and early drought warnings [1-5]. Generally expressed in gravimetric units (g/cm^3) or volumetric units (cm^3cm^{-3}), SM can be defined as the ratio of the total volume of water present in the unsaturated soil zone to the total volume of soil. According to the World Meteorological Organization, SM has been declared as an Essential Climate Variable (ECV) due to its importance in several hydrological and atmospheric processes [6].

However, SM has a strong influence on soil-vegetation-atmosphere exchanges, and its impact remains particularly high in three major regions of the world: the Great Plains of North America, India, and Sahel region, where precipitation is very strongly influenced by SM [2,4,5]. Indeed, several studies have been carried out to properly estimate this variable and its influence on soil-atmosphere exchanges [7,8,9].

However, the use of remote sensing [10-17] and land surface modeling [18-21] remain the best techniques to better understand the effects of SM between the atmosphere and terrestrial surfaces.

The potentialities of satellite measurements of SM on a near-global scale began with the Scanning Multichannel Microwave Radiometer (SMMR, C-band 6 GHz) in 1978 [22] and many algorithms based on the inversion of a

radiative transfer model have been developed for SM estimation [23,24].

Since then, several other sensors have been put into orbit such as the Advanced Microwave System Radiometer/Earth Observing System (AMSR/E-EOS) [23,25,26] in 2002. Quantification of SM with this sensor is based on X-band (10.65 GHz) brightness temperatures [10,27,28] or a combination of C-band (6.91 GHz) [29,30] and X-band brightness temperatures [31,32]. Other examples include the Microwave Imaging Radiometer with Aperture Synthesis (MIRAS), the Soil Moisture and Ocean Salinity (SMOS) satellite which provides soil moisture over the terrestrial surfaces and sea salinity over the oceans [33,34], the Soil Moisture Active and Passive (SMAP) which also provides SM and freezes/thaw values across the globe [35,36]. The Advanced SCATterometer (ASCAT) onboard the MetOP weather satellite also provides information on the degree of saturation (relative humidity) for the upper soil layer (up to 5 cm depth) [10,37,38,39].

In addition, global SM data can also be obtained from reanalysis products [40,41,42], and also from operational numerical weather prediction systems [43]. Some of these model-based products assimilate surface observations to improve the quality of SM estimates. For example, the SM-DAS-2 product assimilates ASCAT surface SM retrievals and screen-level air temperature and humidity measurements [44].

In this study, SM products from the SMAP Level 3 (L3), version 4 and 7, and Level 4 version 5 sensors and SMOS version 650 are used. These obtained data include surface soil moisture and root zone SM estimations.

2. Data and Methods

2.1. Study Sites

Geographically, the three areas (Figure 1) are located in the Sahelian zone of Senegal, more precisely in the pastoral zone of the Ferlo for the Loumbi (15°72 N and 15°01 W) and Bawdi sites (16°02 N and 14°94 W) and in the groundnut basin at Niakhar (14°49 N and 16°46 W) for the third site. The climate of these sites is characterized by two distinct seasons: (i) a short rainy season from July to October and (ii) a long dry season from November to June. From 1950 to 1984, the total annual rainfall gradually decreased, according to [45,45,46,47] leading to a long and dry period [45,46].

The Ferlo, a sub-basin of the Senegal River, is a vast expanse of shrubby steppes and typically Sahelian savannahs south of the Senegal River valley [45]. This area, which straddles five administrative regions (Diourbel, Louga, Matam, Saint-Louis, and Tambacounda), extends approximately between latitudes 16°15 and 14°30 North and longitudes 12°50 and 16°01 West [46]. Its surface area varies according to the authors from 56,269 km^2, i.e. approximately 28% of the national territory, to 60,000 km^2 or 70,000 km^2, which makes it one of the largest eco-geographical zones in Senegal [45,46].

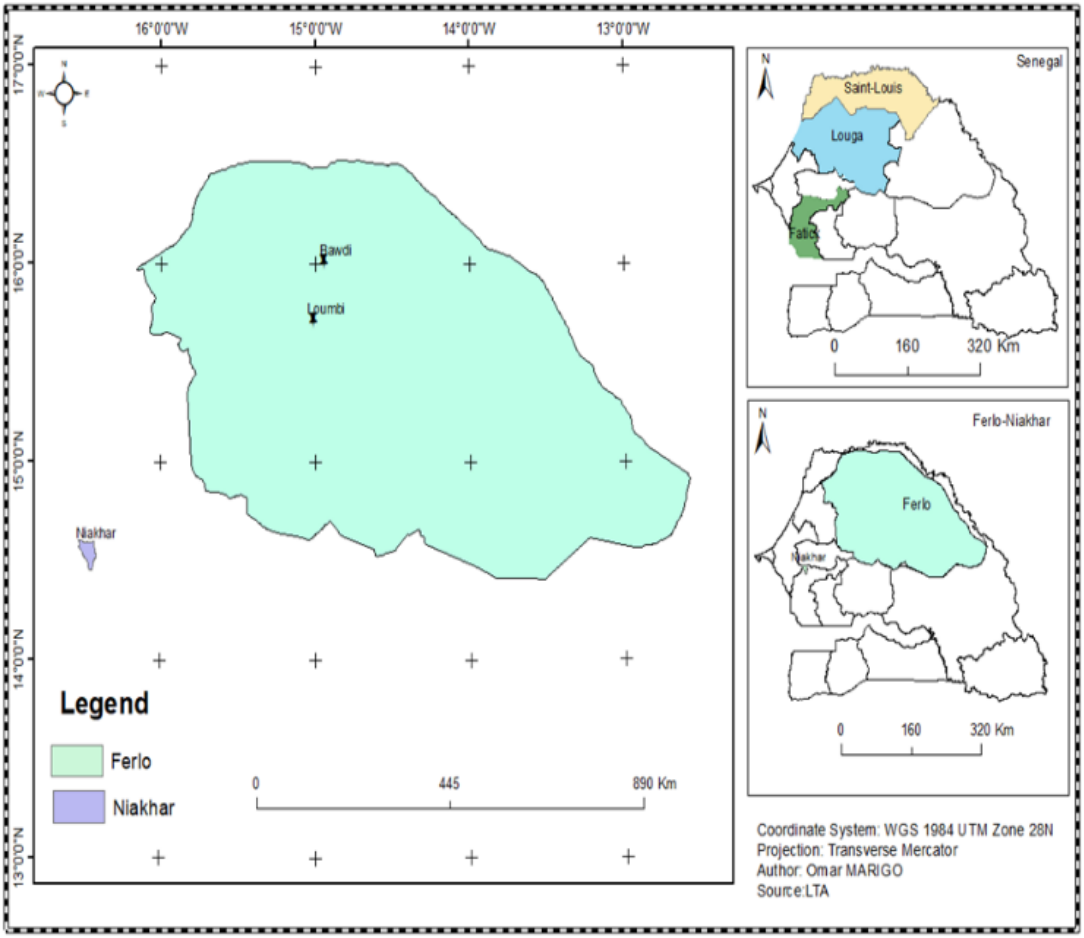

Figure 1. Location of the three sites in the study area (Ferlo: Bawdi and Loumbi; Niakhar)

The soil map of the Ferlo is dominated by sandy textured soil [45,46]. The reliefs are separated by longitudinal depressions with greyish sandy-clay soil, locally chalky and hydromorphic soil with temporary waterlogging, as well as sub-arid brown-red soil. Annual rainfall in the Ferlo is between 200 and 500 mm, associated with high interannual variability (coefficient of variation: 30 to 40%), low relative air humidity in the dry season, and high during the rainy season (annual average of around 35%), high air temperatures (annual average of 29°C), high evaporation (1800 to 2200 mm/year) and precariousness of soil water reserves [46,48,49].

The Niakhar site is located in the administrative region of Fatick, down the groundnut basin of Senegal. It is characterized by a tropical Sudanian climate with rainfall varying between 600 and 900 mm per year on average. Minimum air temperatures range from 21°C to 22°C, while maximum air temperatures range from 35°C to just over 36°C. The soils of the region belong to main 4 types: tropical ferruginous soils (Dior and Deck), hydromorphic soils of the valleys, holomorphic soils **(**saline or "tanne" soils), and mangrove soils found in the islands and estuaries. The region's landscapes are highly artificial, with a predominance of rain-fed farming areas (84%) (CSE: Centre de Suivi Ecologique, 2015).

2.2. Description of Used Data

The data for this study is composed of field SM measurements and SM products derived from SMAP (Soil Moisture Active and Passive), SMOS (Soil Moisture Ocean and Salinity) sensors, and precipitation data from CHIRPS (Climate Hazards Group Infrared Precipitation with Stations) sensors.

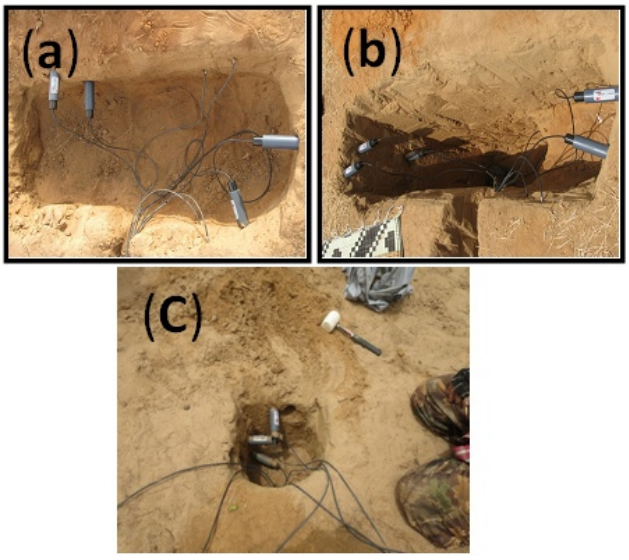

Figure 2. Installation of soil moisture and temperature sensors at: (a)-Bawdi, (b)-Loumbi and (c)-Niakhar

2.2.1. In Situ Measurements

The in-situ data are obtained from SM ML2 Theta Probe (TP) sensors buried underground at different depths (Figure 2, Table 1). These probes are sensitive to the variation of the soil dielectric constant which is then converted into SM via a calibration relationship, the latter being a function of the soil type [50]. The sensors automatically record SM and temperature measurements with a fifteen minutes step. For the three study sites with sandy soil (> 90% sand), we applied the calibration provided by the manufacturer:

$$SM_1 = \frac{100}{a1} * 4.70 * \left(\frac{s_1}{1000}\right)^3 - 6.40 * \left(\frac{s_1}{1000}\right)^2 + 6.40 * \left(\frac{s_1}{1000}\right) - a_0 + 1.00 \quad (1)$$

With SM_1: calibrated soil moisture; s_1= raw data; a_0=1.6 and a_1 =8.4 (a_0 and a_1 are the calibration constants).

In this study, we set up ML2 probes at different depths at the three study sites (Table 1). Subsequently, the 5 cm and 10 cm depth probes were used in the Ferlo (Bawdi and Loumbi) and Niakhar respectively for the evaluation and analysis of SMAP surface soil moisture products with resolutions of 36 km (SPL3SMP), 9 km (SPL3SMP_E), and 9 km (SPL4SMGP_5). All the other depths are used in the estimation and validation of the root zone SM at the Loumbi and Niakhar sites.

Table 1. Site names, number of implemented SM sensors, and sites coordinates

Sites	Number of probes/Soil Moisture	Lat/Long	Period of analysis
Bawdi	2	16°02/ 14°94	2015- 2019
Loumbi	6	15°72/ 15°01	2015- 2019
Niakhar	3	14°49/ 16°45	2018- 2019

2.2.2. Satellites Data

Table 2 summarizes the characteristics of the satellite products used, their launch dates, their spatial-temporal resolutions, and their accessibility.

2.2.2.1. SMAP Products

Launched in 2015, with a temporal resolution of 2-3 days, the SMAP radiometer provides daily global soil moisture products that are generated by the SMAP Science Data Processing System (SDS) at JPL (Jet Propulsion Laboratory) [12,51,52,53].

The estimation of soil moisture from surface Brightness Temperature (BT) measurements is based on the inversion of the radiative transfer equation, commonly known as the tau-omega model of soil moisture by passive microwaves [54].

The SDS provides three types of soil moisture products at different spatial resolutions with an accuracy of 0.04 m^3/m^3:

- The level 3 products (SPL3SMP) with a spatial resolution of 36 km x 36 km. They are derived from the SMAP Level-1C TB (L1C_TB) product which contains the calibrated, geo-located, and time-ordered L1B_TB brightness temperatures that have been resampled to the fixed 36 km grid EASE2.0 (Equal-Area Scalable Earth Grid, Version 2.0) [54,55]. To obtain an accurate estimate of soil moisture, several auxiliary data sets are used. These auxiliary data sets include surface temperature, the

optical thickness of vegetation, simple scattering albedo of vegetation, surface roughness information, land use type, soil texture, and data indicators for identification of land, water, precipitation, urban areas, mountainous terrain, and dense vegetation [54,56,57].

- Enhanced level 3 products (SPL3SMP_E) with a spatial resolution of 9 km x 9 km [54]. This product is a daily SMAP Level-2 (L2) soil moisture composite that is derived from interpolated SMAP Level-1C (L1C) brightness temperatures. Backus-Gilbert's optimal interpolation techniques are used to extract information from the SMAP antenna temperatures and convert them to brightness temperatures, which are displayed on the 9 km x 9 km Elementary Earth Grid, version 2.0 (EASE-Grid 2.0) in a global cylindrical projection [54].
- Level 4 Surface and Root-Zone Soil Moisture data (L4_SM) which provide a surface (0-5cm) and root-zone (0-100cm) soil moisture estimates at 9 km x 9 km resolution [58,59]. Data generated using a terrestrial data assimilation system that combines the advantages of spatial measurements of L-band brightness temperatures, precipitation observations, and land surface modeling. The L4_SM data are therefore generated and distributed on the global grid, cylindrical at 9 km resolution (Equal-Area Scalable Earth, version 2 EASE_2) [59].

2.2.2.2. SMOS Products

The SMOS (Soil Moisture and Ocean Salinity) satellite is an Earth exploration mission of the European Space Agency (ESA) in collaboration with the French National Space Agency (CNES) and the Spanish Centre for the Development of Industrial Technology (CDTI) [33,60,61]. Launched in November 2009, it was the first radiometer operating at L-band (1.4 -2 GHz) [62,63,64,65]. Its main objective is to provide global surface soil moisture at a depth of 0-5 cm, with a spatial resolution of 0.25° x 0.25°, a revisit time of fewer than 3 days, and an accuracy of 0.04 m^3/m^3 [62].

In the present study, the SM data sets available at the CATDS (Centre de Traitement des Données SMOS) are used. The CATDS consists of an operational processing center (C-PDC at IFREMER) and a SM C-EC at the CESBIO (Centre d'Etudes Spatiales de la Biosphère), Toulouse [66]. The objective of CATDS is to produce and distribute level 3 and 4 products, to propose the improvement of level 2 soil moisture algorithms using temporal information (level 3), and to produce higher level datasets from the combination of SMOS data with physical models or other remote sensing products (level 4) to estimate root zone SM. The data used is available in the link In Table 2.

2.2.2.3. Rainfall Products: CHIRPS

CHIRPS (Climate Hazards Group Infrared Precipitation with Stations) is a near-global rainfall data set of over 40 years [67]. CHIRPS integrates satellite images with a spatial resolution of 0.05° x 0.05° with in situ station data to create gridded precipitation time series for trend analysis and seasonal drought monitoring.

The CHIRPS algorithm includes the following steps [67,68,69]: (a) derive TIR (Thermal Infrared) precipitation estimates from near-global geostationary satellite observations, which are generated using local regressions between the multi-satellite pentad tropical precipitation mission and the Cold Cloud Duration (CCD); (b) converting the TIR to percentage anomaly and multiplying by CHPclim (Climate Hazards Group Precipitation Climatology), producing unbiased precipitation fields. Step (a) yields the CHIRPS product, which is a time series back to 1981 at a spatial resolution of 0.05° latitude/longitude. Table 3 summarizes the annual rainfall totals from 2015 to 2019 at the different study sites.

2.3. Methods

SM products from SMAP and SMOS microwave sensors are evaluated at different temporal and spatial scales; in situ measurements served as a reference and are used in the evaluation of soil moisture from microwave products and precipitation data are used to delineate the existing seasons in Senegal. The analysis is organized in three steps:

i) A study of the seasonality of in situ SM observations overall sites from 2017 to 2019 with measurements recorded at 5, 10, 20, 40, and 100 cm depth. For the three validation sites, the 5 cm depth probe measurements are compared with the satellite sensor products for the study of surface moisture and the 10, 20, and 100 cm depths for the SM of the root zone.

ii) For the three study sites, the 5 cm depth probe measurements are compared with the satellite surface SM products (SPL3SMP, SPL3SMP_E, SPL4SMGP_5, SMOS) over five years and a statistical study is carried out to assess their performances.

iii) SMAP L4_SM products and SMOS L4_RZSM products are evaluated at the Loumbi and Niakhar sites taking into account the integrated soil moisture of the root zone (0 - 100 cm).

Table 2. The set of satellite sensors used and their characteristics

Satellites	Period	Spatial Resolution	Time Resolution	Accessibility
SMAP 36km	2015- Current	36 x 36 km	2 to 3 days	https://lpdaacsvc.cr.usgs.gov/appeears/
SMAP 9km	2015- Current	9 x 9 km	2 to 3 days	https://lpdaacsvc.cr.usgs.gov/appeears/
SMOS	2009- Current	0.25° x 0.25°	2 to 3 days	https://www.catds.fr/Products/Available-products-from-CPDC
CHIRPS	1981- Current	0.05° x 0.05°	1 day	Google Earth Engine Platform

Table 3. Annual rainfall totals from 2015 to 2019 in mm

Annual Rainfall (mm)			
Period	Bawdi	Loumbi	Niakhar
2015	265	311	----
2016	268	----	----
2017	204	252	----
2018	250	289	415
2019	162	197	448

The estimation of SM products from satellite sensors was carried out by taking into account only the morning orbits (descending 6 / Am). Indeed, many studies have shown that measurements made in the morning are of better quality than those acquired in the afternoon [70,71,72]. In the morning, the soil is close to water balance and the SM is very representative of the water content of the deeper layers [71,73].

To evaluate and compare the performance of the products used four metrics-widely used by any scientists the study of SM [20,74,75] are deployed: the Pearson's correlation coefficient (R), the Root Mean Squared Error (RMSE, m^3/m^3), the Mean Absolute Error (MAE, m^3/m^3) and the bias (m^3/m^3) defined as below:

$$R = 1 - \frac{\sum_{i=1}^{n}\left(\theta_i - \hat{\theta}_i\right)^2}{\sum_{i=1}^{n}\left(\theta_i - \bar{\theta}\right)^2} \quad (2)$$

$$Bias = \frac{\sum_{i=1}^{n}\left(\hat{\theta}_i - \theta_i\right)}{N} \quad (3)$$

$$RMSE = \sqrt{\frac{\sum_{i=1}^{n}\left(\hat{\theta}_i - \theta_i\right)^2}{N}} \quad (4)$$

$$MAE = \frac{\sum_{i=1}^{n}\left(\left|\hat{\theta}_i - \theta_i\right|\right)}{N} \quad (5)$$

Where $\hat{\theta}_i$ is the satellite soil moisture measurement; $\bar{\theta}_i$, the average of satellite soil moisture measurements; θ_i the in-situ soil moisture measurement and N, the total number of samples taken into consideration.

3. Results and Discussion

3.1. In Situ Temporal Variations of SM

Figure 3 and Figure 4 show the temporal evolution of soil moisture measured at different depths profiles (5, 10, 20, 40, and 100 cm) and rainfall at the three study sites (Bawdi, Loumbi, and Niakhar) from 2017 to 2019. The lack of data from the Niakhar site is due to technical problems. An increase in SM can be noted for all probes from the first rains except for the 40 and 100 cm depth probes in Loumbi and the 20 and 40 cm depths in Niakhar.

For years of study, there is an increase in moisture in all probes from the first rains except for the 40 and 100 cm depths in Loumbi (Figure 3 (a1 and a2)) and the 20 and 40 cm depths in Niakhar (Figure 4(c1 and c2)). At the Bawdi site (Figure 3 (b1 and b2)), all probes reacted as the first rains fell, and this continued for the entire study period. These results demonstrate the performance of the ML2 probes in measuring soil moisture values at different depths. The 40 cm probe at Loumbi records an increase in humidity from August onwards, unlike the 100 cm probe, which reacts in mid-September.

This is consistent with the infiltration time of soil moisture during the rainy season. Thus, the recorded SM follows the seasonality since in the dry season they do not show significant increases. On the other hand, in the rainy season, we see distinct responses of the in-situ sensors to the acquisition of SM. We also note that in the dry season, the moisture values at depths of 40-100 cm at the Loumbi site are much higher than the moisture values measured at depths of 5 and 10 cm.

At Niakhar, three probes at depths of 10, 20, and 40 cm are installed. The measurements recorded by these probes in the rainy season show that they follow the dynamics of the existing seasons in the area. The probe installed at 40 cm records soil moisture measurements just after the 10 and 20 cm probes; this indicates faster infiltration. This may be the result of a soil difference or the plowing effect that facilitates the infiltration of rainwater. In fact, in the Niakhar site, which is an agricultural area, the soil is plowed at the first rains come, which makes it more permeable to water.

3.2. Comparative Analysis of SMAP and SMOS SM Products

In both Bawdi and Loumbi sites, there are two probes of 5 cm depth, only the probe installed at a depth of 5 cm with the smallest standard deviation is used by the site to evaluate SMAP and SMOS satellite products and the 10 cm probe is used in Niakhar.

Figure 5 shows the seasonal variation of the different SM products (SMAP at 9-36 km resolution and SMOS at 0.25° x 0.25°) in comparison with in situ data. The statistical scores are presented in Table 4. Comparing annually the soil moisture results, the highest correlation coefficient is found in the Bawdi site in 2016 where R is equal to 0.96 between the SPL3SMP sensor and field measurements. In Loumbi, the highest correlation score was recorded between the SPL3SMP_E sensor and field measurements, where R was 0.94 in 2018. 0.89 is the highest correlation coefficient recorded between the SPL3SMP_E sensor and field measurements in Niakhar in 2019.

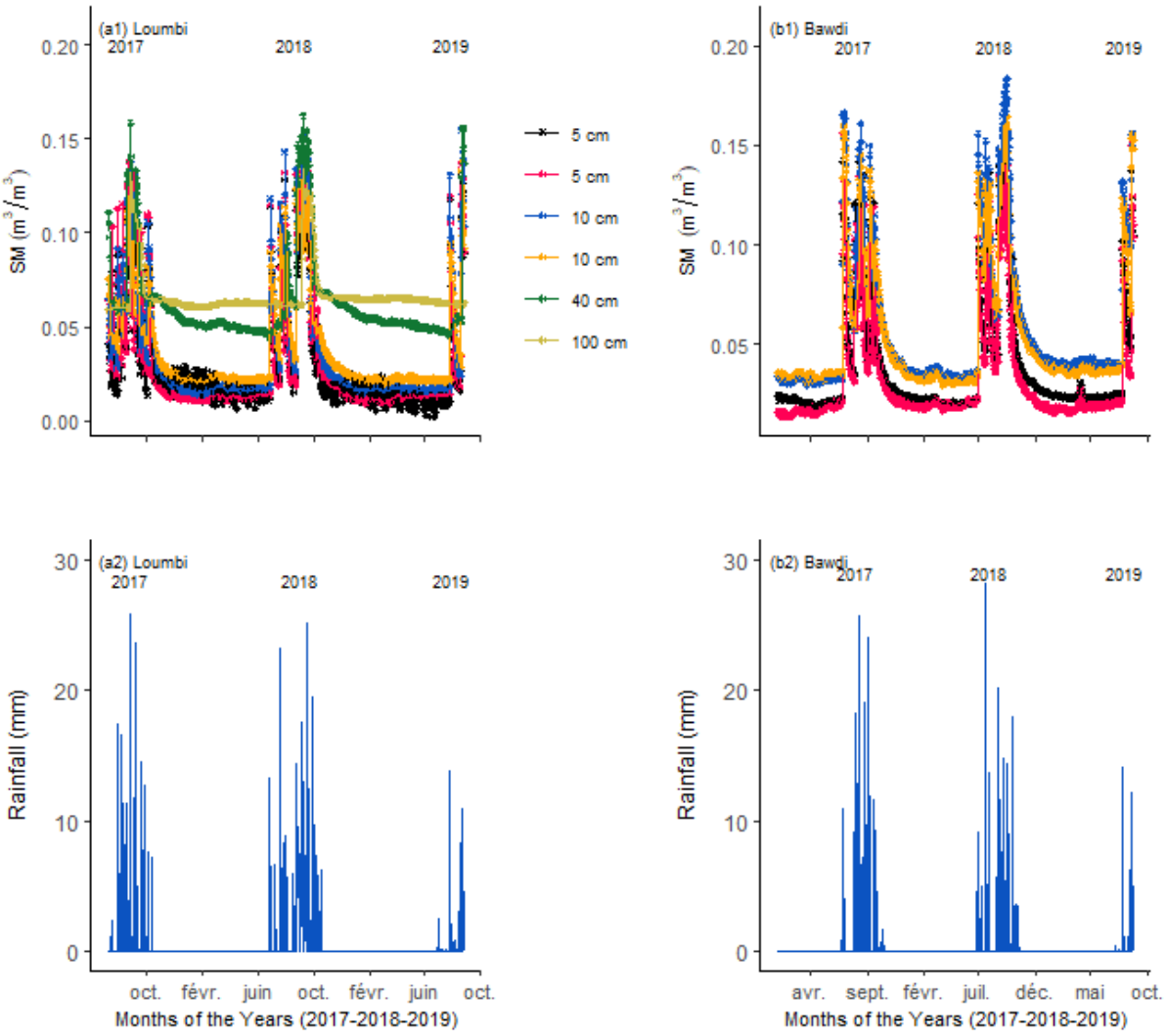

Figure 3. Time series of in situ SM measured at different depths at (a) Bawdi, (b) Loumbi sites over the 2017 – 2019 period: Pastorale zone

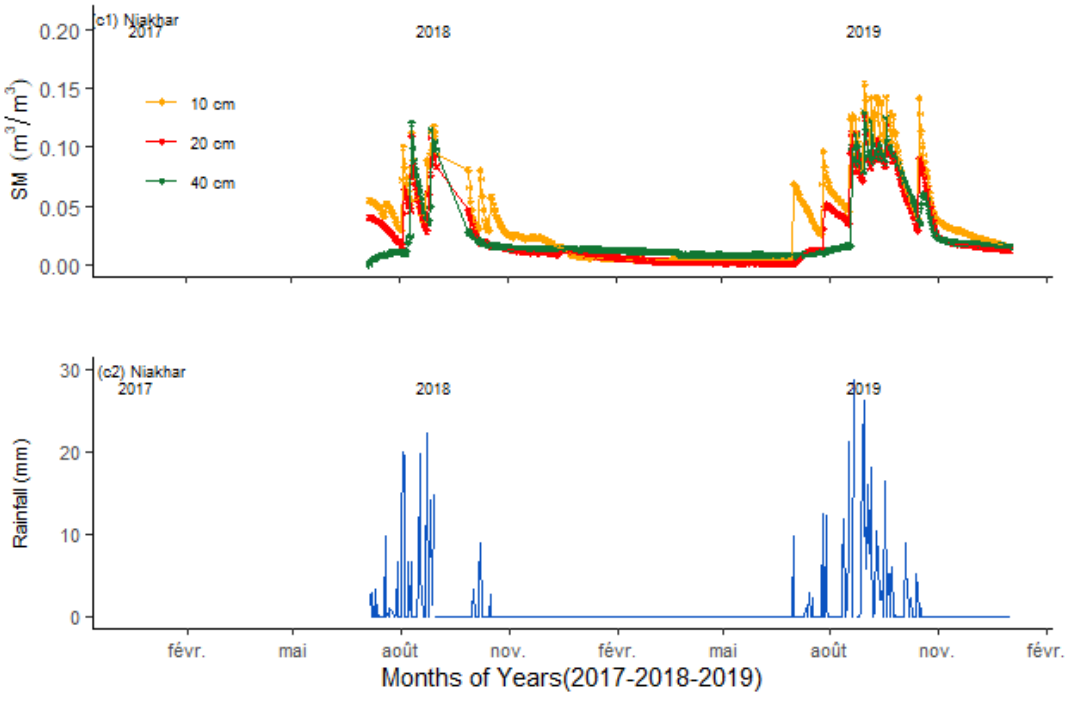

Figure 4. Time series of in situ SM measured at different depths at (c) Niakhar site over the 2017 – 2019 period: agricultural zone

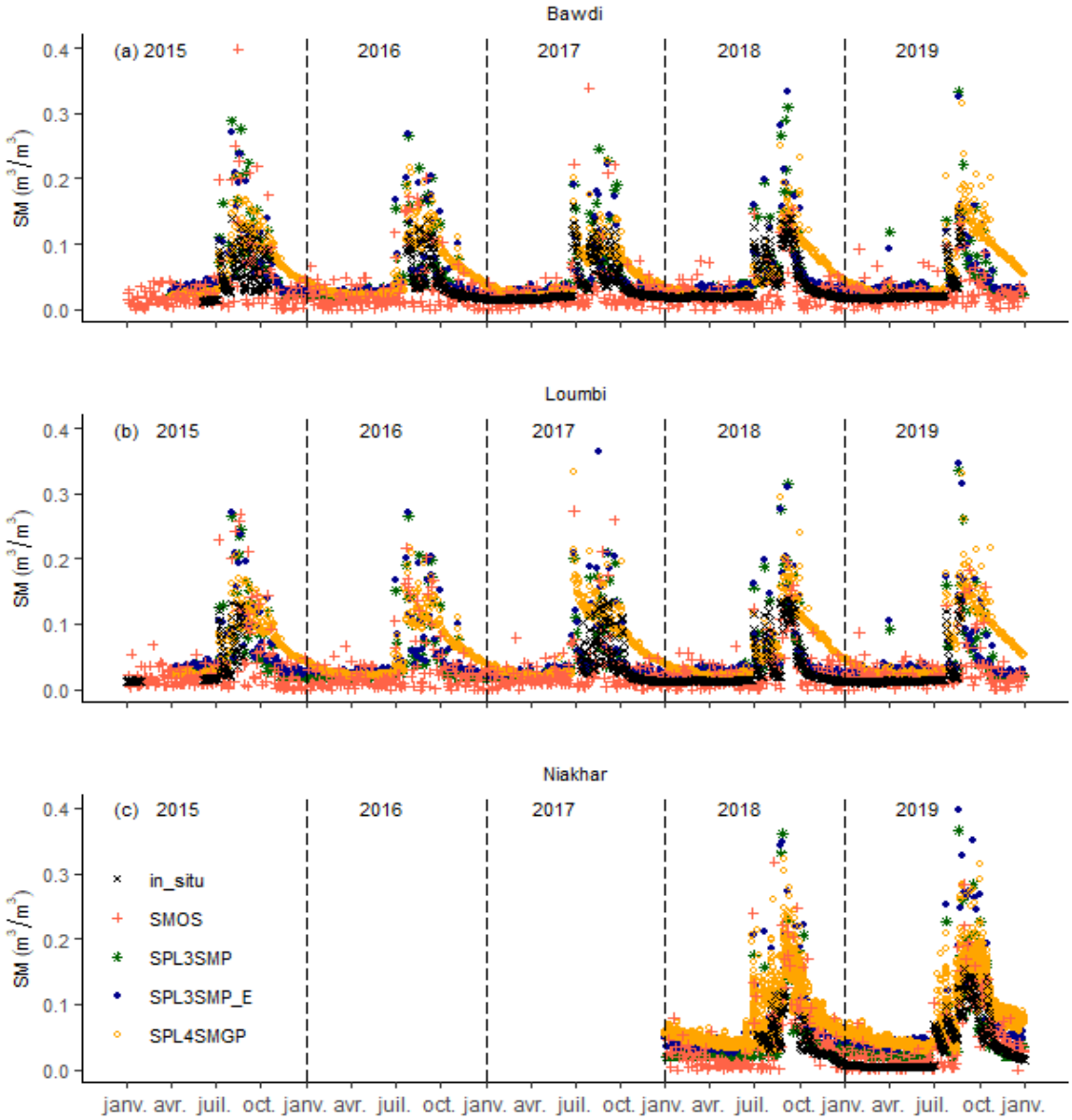

Figure 5. Temporal variation of SMAP, SMOS, and in-situ SM data at (-a) Bawdi, (b) Loumbi) and (c) Niakhar sites

In the three sites, at the end of the rainy season, Bawdi (Figure 5a), Loumbi (Figure 5b), and Niakhar (Figure 5c), the soil moisture values of the microwave sensors decrease to their minimum which is close to 0.02 m^3/m^3 and the in-situ observations decrease to 0.01 m^3/m^3.

This drop lasts from January to the end of June. In fact, the end of the dry season is accompanied by dry winds and high temperatures [56,76], which accelerate the drying out of the soil, leading to a more rapid decrease in soil moisture. The SMAP products (SPL3SMP and SPL3SMP_E) remain quite high in the rainy season and can reach maxima of 0.3 m^3/m^3 soil moisture compared to the SMAP Level 4 (SPL4SMGP_5), SMOS, and in situ products. The observations of the SPL4SMGP product are marked by a progressive decrease in soil moisture at the end of the rainy season in contrast to the other products of the two satellites studied and the field measurements. This shows either a strong sensitivity of the SMAP products to low humidity or sensitivity to other unidentified seasonal phenomena. The SMOS measurements, on the other hand, are much more scattered, especially during the dry season.

These results corroborate studies done in another site in the Ferlo, namely Dahra [77] about 80 km south of the Loumbi and Bawdi sites. They also confirm results from other areas of the Sahel, specifically Mali, Benin, and Niger among others [16,22,25,48,78,79]. This demonstrates that these L-band satellites are sensitive to the spatial-temporal dynamics of the amount of water in the soil. This moisture is strongly governed by fluctuations in rainfall, temperature, evapotranspiration, and other intrinsic soil parameters [37,80].

In Niakhar, the values of the satellite products reflect the dynamics of two existing seasons. Compared to the sites in the Ferlo, the peak of soil moisture is reached in September. The microwave measurements are much higher than the field measurements. This may mean that the satellite products recover soil moisture data better than the in-situ measurements.

The correlation between the in-situ measurements and the satellite products allows a better assessment of the accuracy of the soil moisture of the SMAP and SMOS sensors. Initially, only data at 5 cm depth were considered in this section (Figure 6, Figure 7, and Figure 8).

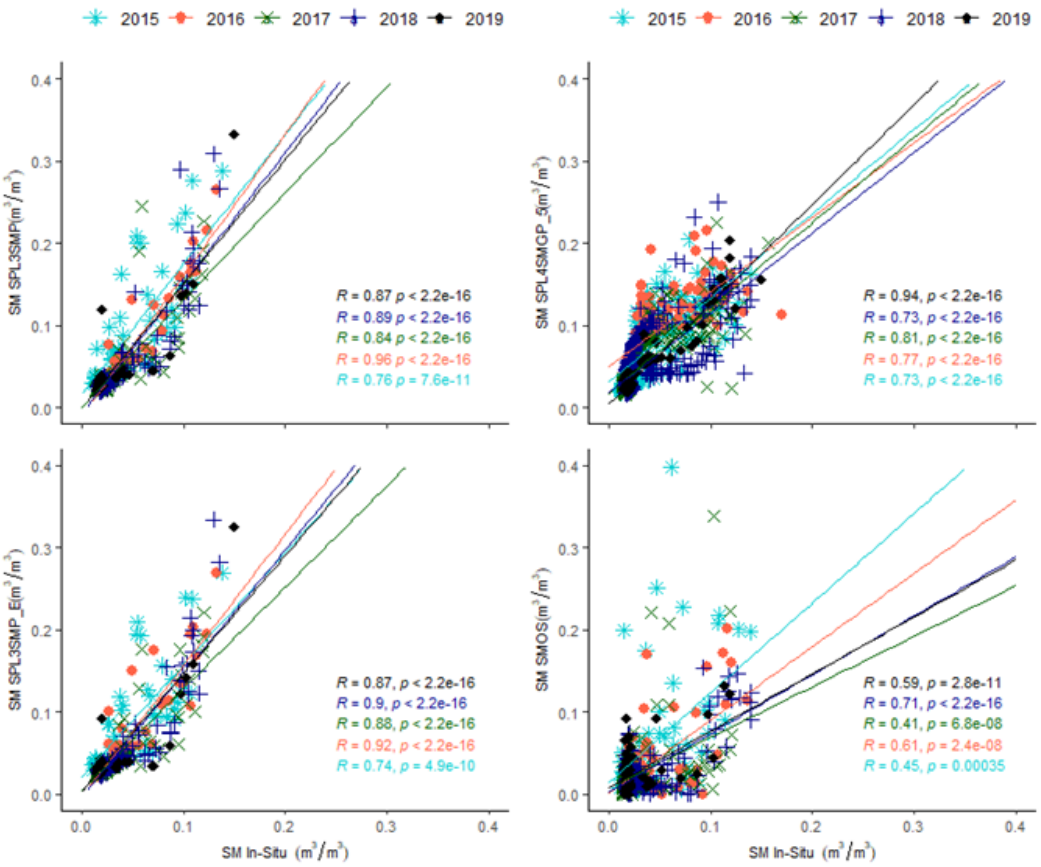

Figure 6. In situ SM versus SMAP and SMOS SM products in Bawdi site

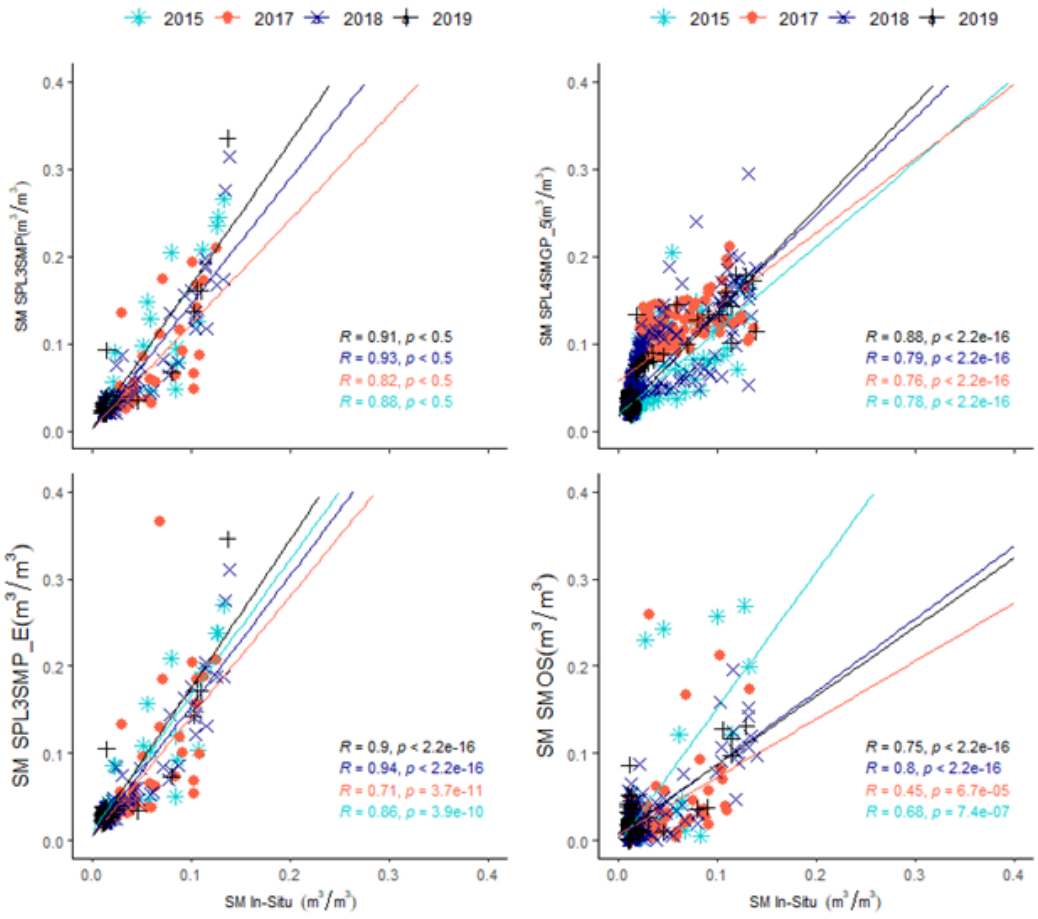

Figure 7. In situ SM versus SMAP and SMOS SM products Loumbi site

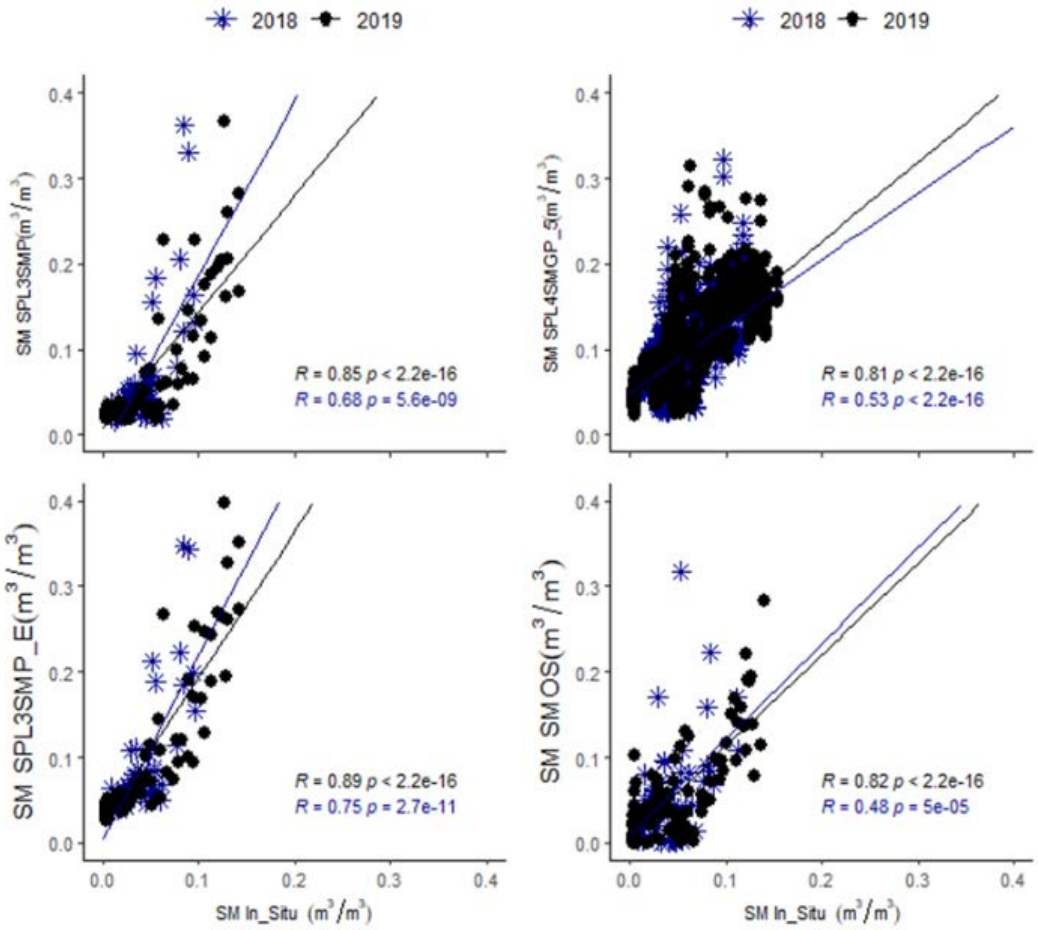

Figure 8. In situ versus SMAP and SMOS SM products at Niakhar site

- **Bawdi Site**

Figure 6 shows the scatter plot between satellite products and in situ SM for the period 2015-2019. We generally notice a good correlation between the SMAP products of the SPL3SMP level 3 sensor, version 7 with a spatial resolution of 36 km, and the in-situ SM with a correlation coefficient that varies over the five years between 0.76 and 0.96. With an RMSE smaller than 4% m3/m3 for all years except 2015 (RMSE= 0.06 m^3/m^3) according to Table 4, confidence in the quality of the estimates of the different products is very high. Thus, despite its very low resolution of 36 km, the SPL3SMP products can reproduce in-situ SM at this site.

Furthermore, the annual correlation between the 9 km resolution product (SPL3SMP_E) of SMAP and the in-situ SM is high and ranges from, 0.74 to 0.92. Except in 2015 when the RMSD is 0.05 m3/m3, the other years have an RMSE lower than 0.04 m3/m3. This shows the good performance of the SMAP sensor in estimating SM values.

For the SPL4SMGP_5 9 km SMAP and SMOS sensors, the correlation coefficients range between 0.73-0.94 and 0.45-0.71, respectively (Table 4). The Bias values are also low for all sensors over the five years of study.

- **Loumbi Site**

In Loumbi (Figure 7), the study period is four years (2015, 2017, 2018, and 2019). Due to technical problems, we did not have data from 2016. The scatterplots for the Loumbi site are quite similar to those for Bawdi. Table 4 shows the statistical results between the microwave sensor products and the ground measurements.

For the SMAP SPL3SMP sensor, we observe a good correlation with a correlation coefficient R between 0.86 and 0.93. The same remarks can be made as for the SPL3SMP_E sensor of SMAP 9 km where the correlation coefficient varies between 0.86 and 0.94. We also find RMSE below 0.04 m^3/m^3. In addition, the SPL4SMGP sensor products have a very significant correlation while compared to the in-situ measurements with a correlation coefficient greater than 0.5 for all four years of study. However, the SMOS products are well correlated with the ground values, correlation coefficients above 0.5. The results obtained at the Loumbi site showed that the performance of the satellite sensors is very high for estimating SM despite RMSE sometimes exceeding the specifications (0.04 m^3/m^3).

- **Niakhar Site**

Figure 8 shows the scatter plots and Table 4 gives the RMSE, R, MAE, and Bias between all products. It is generally noted that the correlation coefficient varies between 0.48 and 0.89. A good correlation was noted between the SMAP SPL3SMP product and the ground observations between 2018 and 2019. It is also observed that a good part of the measurements is between 0.05 and 0.1 m^3/m^3. The largest correlation coefficient is found between the SMAP SPL3SMP_E product and the ground values where R is equal to 0.89. The results found at the Niakhar site (agricultural area) show that there is a good link between the earth observation data and the in-situ data.

Table 4. Descriptive statistics between observations from SPL3SMP (36km), SPL3SMP _E (9km), SPL4SMGP (9km), SMOS, and in-situ measurements from Bawdi, Loumbi, and Niakhar sites for a depth of 5cm: R, RMSE (in m^3/m^3), MAE (in m^3/m^3) and Bias (in m^3/m^3)

	Products	SPL3SMP 36 km					SPL3SMP_E 9 km					SPL4SMGP_5 9 km					SMOS 0.25°x 0.25°				
Sites	Years	R	RMSE	MAE	Bias	N	R	RMSE	MAE	Bias	N	R	RMSE	MAE	Bias	N	R	RMSE	MAE	Bias	N
Bawdi	2015	**0.76***	0.06	0.04	0.04	51	**0.74***	0.05	0.04	0.04	51	**0.73***	0,04	0.03	0.03	137	0.45	0.07	0.04	0.01	59
	2016	**0.96****	0.03	0.02	0.02	59	**0.92****	0.03	0.02	0.02	59	**0.77***	0.05	0.04	0.04	162	**0.61***	0.04	0.03	-0.003	71
	2017	**0.84****	0.02	0.01	0.01	137	**0.88****	0.02	0.01	0.01	132	**0.81****	0,03	0.02	0.02	365	0.41	0.04	0.02	-0.005	162
	2018	**0.89****	0.03	0.01	0.01	137	**0.90****	0.03	0.01	0.01	136	**0.73***	0.03	0.02	0.01	362	**0.71***	0.02	0.02	-0.008	161
	2019	**0.87****	0.02	0.01	0.01	75	**0.87****	0.03	0.01	0.01	74	**0.94****	0.01	0.01	0.01	237	**0.59***	0.02	0,01	-0.0004	105
Loumbi	2015	**0.88****	0.05	0.04	0.03	32	**0.90****	0.06	0.04	0.04	32	**0.78***	0.03	0.02	0.01	83	**0.68***	0.08	0.03	0.02	43
	2017	**0.82****	0.05	0.02	0.01	66	**0.71***	0.05	0.02	0.02	65	**0.76***	0.05	0.05	0.04	176	0.45	0.07	0.03	-0.0003	73
	2018	**0.93****	0.03	0.01	0.01	137	**0.94****	0.03	0.02	0.02	136	**0.79***	0.04	0.03	0.03	365	**0.80****	0.02	0.01	-0.0005	159
	2019	**0.91****	0.03	0.01	0.01	75	**0.90****	0.03	0.02	0.02	74	**0.88****	0.02	0.02	0.02	237	**0.75***	0.01	0.01	0.004	105
Niakhar	2018	**0.68***	0.06	0.03	0.02	57	**0.75***	0.07	0.05	0.05	57	**0.53***	0.05	0.04	0.04	153	0.48	0.05	0.03	0.01	64
	2019	**0.85****	0.04	0.02	0.02	123	**0.89****	0.06	0.04	0.04	122	**0.82****	0.05	0.04	0.03	365	**0.82****	0.03	0.02	0.01	155

3.3. Global Estimates of all Satellite Products versus in Situ Measurements

A site-by-site and global study between the measurements of the products from the satellite sensors and the ground observations were made and the results are shown in Figure 9. Figures 9a, 9b, and 9c show the Bawdi, Loumbi, and Niakhar sites respectively. It is generally noted that many measurements are between 0.01 and 0.15 m^3/m^3. By grouping, all the measurements from all the sensors, a good correlation between satellite observations and field measurements can be observed at all sites.

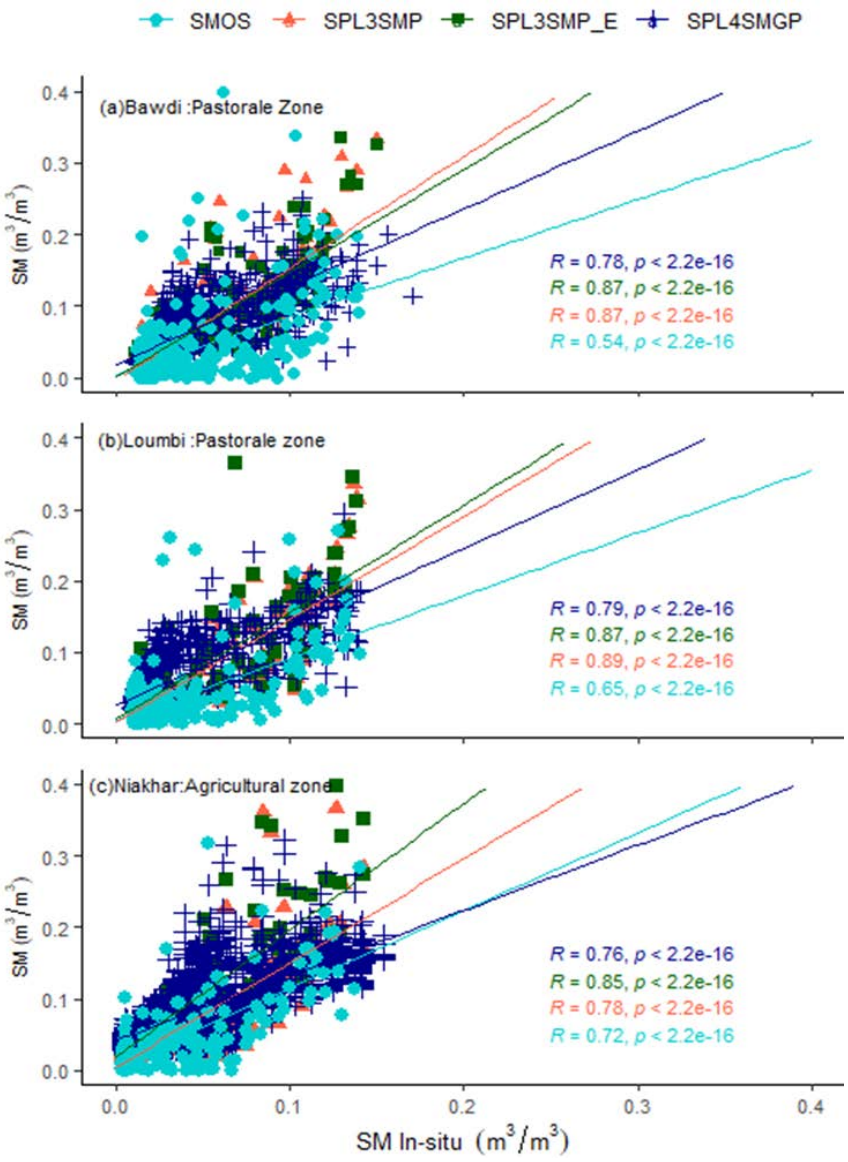

Figure 9. Global interpretation between satellite products and in situ measurements: (a) Bawdi, (b) Loumbi, and (c) Niakhar

Table 5. Soil moisture scores of all sites between satellite measurements versus in situ measurements

Soil moisture scores	SPL3SMP			SPL3SMP_E			SPL4SMGP_5			SMOS		
	R	RMSE	Bias	R	RMSE	Bias	R	RMSE	Bias	R	RMSE	Bias
(a) Bawdi	**0.87**	0.03	0.02	**0.87**	0.03	0.02	**0.78**	0.03	0.02	0.54	0.04	-0.002
(b) Loumbi	**0.89**	0.04	0.02	**0.87**	0.04	0.02	**0.79**	0.04	0.03	0.65	0.04	0.03
(c) Niakhar	**0.78**	0.05	0.02	**0.85**	0.06	0.05	**0.77**	0.05	0.04	0.72	0.03	0.01

Table 5 gives the R, RMSE, and Bias between satellite and in situ measurements. This may mean that soil and climatic characteristics do not have a great influence on the recovery of soil moisture measurements. With the SMAP products, a good correlation was respectively found at Bawdi where the correlation coefficient R is between 0.78 and 0.87 and RMSEs below the specifications (0.04 m^3/m^3); for SMOS, R is equal to 0.54, RMSEs < 0.04 m^3/m^3. At Loumbi where R is between 0.79 and 0.89 for SMAP measurements and 0.65 for SMOS measurements. These two sites together give Ferlo which has similar scores to these two different sites, 0.77 < R < 0.89.

In Niakhar, very good results were also obtained with all satellite sensor products as the correlation coefficient is between 0.77 and 0.85 for SMAP and 0.72 for the SMOS product. The results obtained in the Ferlo (silvopastoral zone) corroborate the results of [45].

4. Validation of Soil Moisture in the Root Zone

4.1. Loumbi: Pastoral Area

Figure 10 shows the temporal dynamics of soil moisture from 2018 to 2019. Integrated moisture with depths of 5, 10, 40, and 100 cm is calculated to have an in-situ root zone soil moisture. This calculated moisture is compared to the moisture of the SMAP and SMOS sensors in the root zone. Generally, all observations reflect the seasonal dynamics, i.e., the two seasons can be distinguished. However, there are also differences between the SMAP values and the other types of measurements, especially during the dry season. The SMOS curve is above all other curves; this could indicate that this sensor overestimates the soil moisture measurements of the root zone.

4.2. Niakhar: Agricultural Areas

Figure 10 also shows the temporal soil moisture dynamics of the root zone of the satellite products and the in-situ measurements at Niakhar. This site is in an agricultural environment with soil that is constantly plowed. There is a difference in the variation of moisture values from the microwave sensors compared to the Loumbi site. Here, the difference in values is noted between the satellite and in-situ products especially during the dry season when the microwave observations are significantly higher. In September 2018, in the middle of the rainy season, the soil moisture variations of the SMAP sensor are much higher than the other measurements with a peak above 0.3 m3/m3. This can be justified by the intensity of the rainfall and the capacity of the soil to infiltrate. In agricultural areas, water infiltration is favored by anthropogenic activities in the soil.

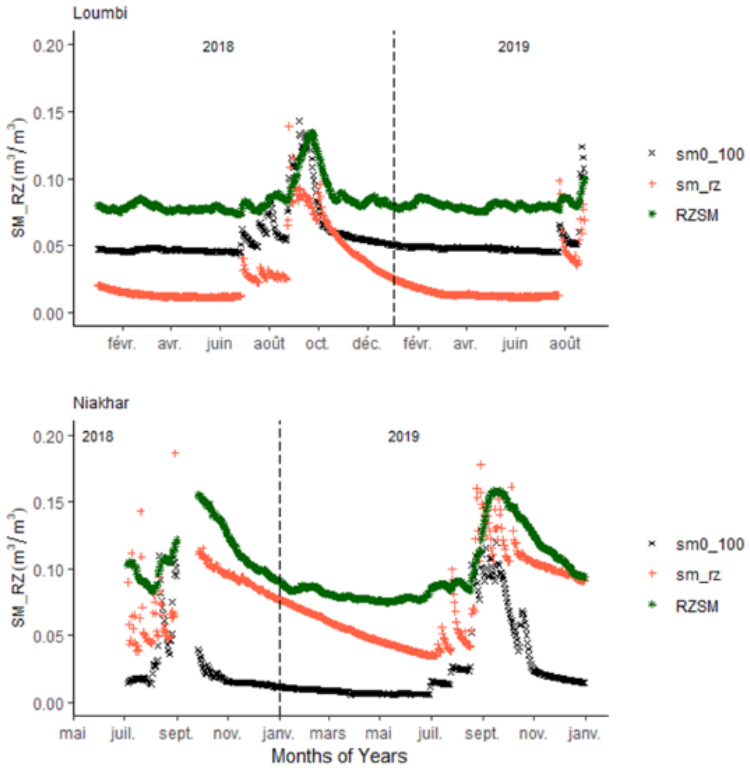

Figure 10. Spatial-temporal variation of SM of the root zone in a silvopastoral area (Loumbi) and an agricultural area (Niakhar)

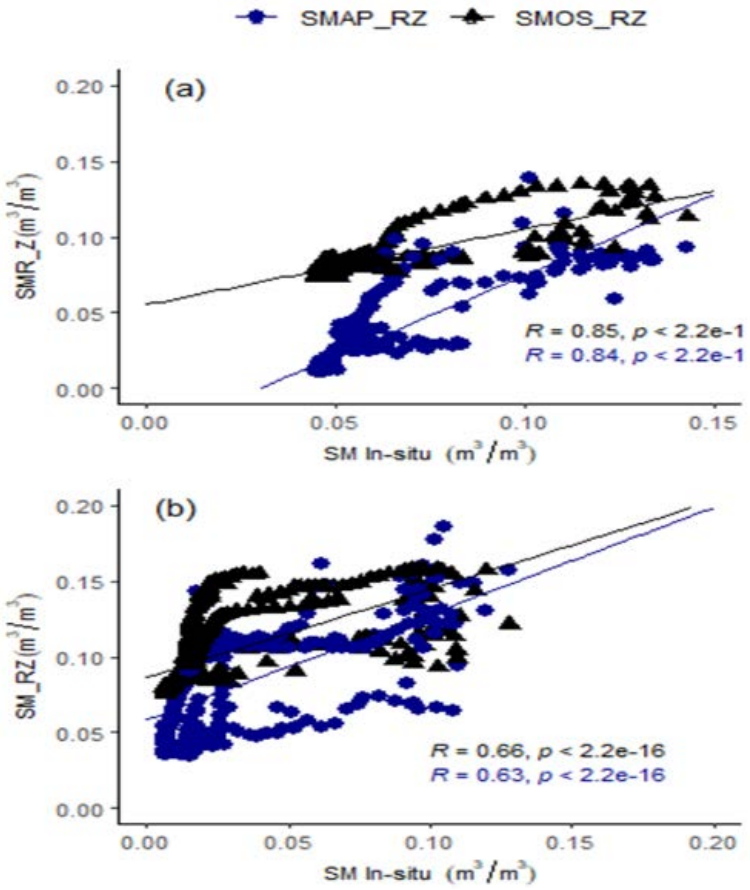

Figure 11. Comparison between microwave sensor products and in situ root zone soil moisture measurements: (a) Loumbi and (b) Niakhar

Table 6. Correlation coefficient, RMSD, MAE, and Bias between the root zone soil moisture of the SMAP_RZ resolution 9 km, SMOS_RZ sensors, and the in-situ soil moisture in Loumbi and Niakhar

SM scores	SMAP_RZ			SMOS_RZ		
	R	RMSE	Bias	R	RMSE	Bias
Loumbi	**0.85**	0.03	-0.03	**0.84**	0.03	0.03
Niakhar	**0.63**	0.05	0.05	**0.66**	0.08	0.07

Figure 11(b) shows the scatter plots and Table 6 the scores between the different products. A good correlation was found where the correlation coefficient is equal to 0.84 for SMAP_RZ and 0.85 for SMOS_RZ. This demonstrates the good performance of SMAP and SMOS in taking SM measurements of the root zone.

5. Conclusion

In this study, a multi-year evaluation of various SM microwave products of the surface (5 cm) and the root zone (0-100 cm) soil layers was carried out over three sites located in Senegal. Overall, the results obtained in this study corroborate the results found by previous studies in the Sahelian zone [15,16,76].

Microwave sensors that scan the first few centimeters of soil depth (5cm) have products that have mostly good correlation and RMSEs that are often below specifications, i.e., 0.04 m3/m3 in a pastoral area: Loumbi and Bawdi. Therefore, the products of SMAP and SMOS sensors, with high correlation coefficients in these two sites, can be good indicators of surface soil moisture. Similarly in the agricultural site of Niakhar, satellite results and situ surface measurements show the sensitivity of the sensors in the agricultural area.

Due to lack of data at the Bawdi site, root zone estimates were made at Loumbi and Niakhar with the SPL4SMGP 9 km sensor from SMAP_RZ and the SMOS_RZ sensor from SMOS. A very large result was found at Loumbi with RMSEs mainly less than or equal to 0.04 m3/m3. The results found at the Niakhar site also show the importance of microwave sensors on the recovery of soil moisture measurements from the root zone. Thus, this work shows the sensitivity of in situ and satellite sensors on L-band soil moisture recovery.

Nevertheless, further studies are needed to improve the observations of microwave sensors on soil moisture retrieval for better agricultural monitoring in the Sahel, particularly in Senegal.

Acknowledgements

AMMA-CATCH + F. Timouk for help with the installation of the Niakhar probes and O. Roupsard for the maintenance of the Niakhar site. P. Hiernaux, L. Kergoat, F Gangneron for help with the collection of the Loumbi and Bawdi in-situ data.

References

[1] I. Barry, ‘Estimation de l’humidité du sol en milieu agricole par combinaison des données polarimétriques radar en bande C et des

micro-ondes passives en bande L', PhD Thesis, Université de Sherbrooke, 2021.

[2] S. I. Seneviratne *et al.*, 'Investigating soil moisture–climate interactions in a changing climate: A review', *Earth-Science Reviews*, vol. 99, no. 3-4, pp. 125-161, 2010.

[3] R. D. Koster *et al.*, 'GLACE: The Global Land–Atmosphere Coupling Experiment. Part I: Overview', *Journal of Hydrometeorology*, vol. 7, no. 4, pp. 590-610, Aug. 2006.

[4] C. M. Taylor, 'Detecting soil moisture impacts on convective initiation in Europe', *Geophysical Research Letters*, vol. 42, no. 11, pp. 4631-4638, 2015.

[5] C. M. Taylor *et al.*, 'Frequency of Sahelian storm initiation enhanced over mesoscale soil-moisture patterns', *Nature Geoscience*, vol. 4, no. 7, pp. 430-433, 2011.

[6] D. R. Legates *et al.*, 'Soil moisture: A central and unifying theme in physical geography', *Progress in Physical Geography: Earth and Environment*, vol. 35, no. 1, pp. 65-86, Feb. 2011.

[7] W. T. Crow, F. Chen, R. H. Reichle, and Q. Liu, 'L band microwave remote sensing and land data assimilation improve the representation of prestorm soil moisture conditions for hydrologic forecasting', *Geophysical Research Letters*, vol. 44, no. 11, pp. 5495–5503, 2017.

[8] W. T. Crow *et al.*, 'Upscaling sparse ground-based soil moisture observations for the validation of coarse-resolution satellite soil moisture products', *Reviews of Geophysics*, vol. 50, no. 2, 2012.

[9] F. Anctil, C. Michel, C. Perrin, and V. Andréassian, 'A soil moisture index as an auxiliary ANN input for stream flow forecasting', *Journal of Hydrology*, vol. 286, no. 1, pp. 155-167, Jan. 2004.

[10] W. Wagner *et al.*, 'The ASCAT Soil Moisture Product: A Review of its Specifications, Validation Results, and Emerging Applications', *Meteorologische Zeitschrift*, pp. 5-33, Feb. 2013.

[11] W. Wagner *et al.*, 'Temporal Stability of Soil Moisture and Radar Backscatter Observed by the Advanced Synthetic Aperture Radar (ASAR)', *Sensors*, vol. 8, no. 2, Art. no. 2, Feb. 2008.

[12] G. Bloschl, 'Wagner, W., J. Komma, G. Bloschl et al. (2013) The ASCAT soil moisture product: A review of its specifications, validation results, and emerging applications. Meteorologische Zeitschrift, 22, 5-33.

[13] Y. H. Kerr, 'Soil moisture from space: Where are we?', *Hydrogeol J*, vol. 15, no. 1, pp. 117–120, Feb. 2007.

[14] Y. H. Kerr *et al.*, 'The SMOS Soil Moisture Retrieval Algorithm', *IEEE Transactions on Geoscience and Remote Sensing*, vol. 50, no. 5, pp. 1384-1403, May 2012.

[15] F. Baup, E. Mougin, P. de Rosnay, F. Timouk, and I. Chênerie, 'Surface soil moisture estimation over the AMMA Sahelian site in Mali using ENVISAT/ASAR data', *Remote Sensing of Environment*, vol. 109, no. 4, pp. 473-481, Aug. 2007.

[16] S. Louvet *et al.*, 'SMOS soil moisture product evaluation over West-Africa from local to regional scale', *Remote Sensing of Environment*, vol. 156, pp. 383-394, Jan. 2015.

[17] N. Djamai, R. Magagi, K. Goita, O. Merlin, Y. Kerr, and A. Walker, 'Disaggregation of SMOS soil moisture over the Canadian Prairies', *Remote Sensing of Environment*, vol. 170, pp. 255-268, Dec. 2015.

[18] B. W. Barrett, E. Dwyer, and P. Whelan, 'Soil Moisture Retrieval from Active Spaceborne Microwave Observations: An Evaluation of Current Techniques', *Remote Sensing*, vol. 1, no. 3, Art. no. 3, Sep. 2009.

[19] G. P. Petropoulos, P. K. Srivastava, M. Piles, and S. Pearson, 'Earth Observation-Based Operational Estimation of Soil Moisture and Evapotranspiration for Agricultural Crops in Support of Sustainable Water Management', *Sustainability*, vol. 10, no. 1, Art. no. 1, Jan. 2018.

[20] L. Bai, X. Lv, and X. Li, 'Evaluation of Two SMAP Soil Moisture Retrievals Using Modeled- and Ground-Based Measurements', *Remote Sensing*, vol. 11, no. 24, Art. no. 24, Jan. 2019.

[21] K. C. Kornelsen and P. Coulibaly, 'Advances in soil moisture retrieval from synthetic aperture radar and hydrological applications', *Journal of Hydrology*, vol. 476, pp. 460-489, Jan. 2013.

[22] P. de Rosnay *et al.*, 'Multi-scale soil moisture measurements at the Gourma meso-scale site in Mali', *Journal of Hydrology*, vol. 375, no. 1, pp. 241-252, Aug. 2009.

[23] E. G. Njoku, T. J. Jackson, V. Lakshmi, T. K. Chan, and S. V. Nghiem, 'Soil moisture retrieval from AMSR-E', *IEEE transactions on Geoscience and remote sensing*, vol. 41, no. 2, pp. 215-229, 2003.

[24] C. S. Draper, J. P. Walker, P. J. Steinle, R. A. De Jeu, and T. R. Holmes, 'An evaluation of AMSR–E derived soil moisture over Australia', *Remote Sensing of Environment*, vol. 113, no. 4, pp. 703-710, 2009.

[25] T. Pellarin, S. Louvet, C. Gruhier, G. Quantin, and C. Legout, 'A simple and effective method for correcting soil moisture and precipitation estimates using AMSR-E measurements', *Remote Sensing of Environment*, vol. 136, pp. 28-36, Sep. 2013.

[26] R. Bindlish, T. J. Jackson, A. J. Gasiewski, M. Klein, and E. G. Njoku, 'Soil moisture mapping and AMSR-E validation using the PSR in SMEX02', *Remote Sensing of Environment*, vol. 103, no. 2, pp. 127-139, Jul. 2006.

[27] A. Balenzano *et al.*, 'On the use of temporal series of L-and X-band SAR data for soil moisture retrieval. Capitanata plain case study', *European Journal of Remote Sensing*, vol. 46, no. 1, pp. 721-737, Jan. 2013.

[28] M. El Hajj *et al.*, 'Soil moisture retrieval over irrigated grassland using X-band SAR data', *Remote Sensing of Environment*, vol. 176, pp. 202-218, Apr. 2016.

[29] R. D. Koster, Y. Chang, H. Wang, and S. D. Schubert, 'Impacts of Local Soil Moisture Anomalies on the Atmospheric Circulation and on Remote Surface Meteorological Fields during Boreal Summer: A Comprehensive Analysis over North America', *Journal of Climate*, vol. 29, no. 20, pp. 7345-7364, Oct. 2016.

[30] M. Zribi, 'Développement de nouvelles méthodes de modélisation de la rugosité pour la rétrodiffusion hyperfréquence de la surface du sol', PhD Thesis, Toulouse 3, 2030.

[31] M. Owe, R. de Jeu, and T. Holmes, 'Multisensor historical climatology of satellite-derived global land surface moisture', *Journal of Geophysical Research: Earth Surface*, vol. 113, no. F1, 2008.

[32] M. Owe, R. de Jeu, and J. Walker, 'A methodology for surface soil moisture and vegetation optical depth retrieval using the microwave polarization difference index', *IEEE Transactions on Geoscience and Remote Sensing*, vol. 39, no. 8, pp. 1643-1654, Aug. 2001.

[33] Y. H. Kerr *et al.*, 'The SMOS Mission: New Tool for Monitoring Key Elements ofthe Global Water Cycle', *Proceedings of the IEEE*, vol. 98, no. 5, pp. 666-687, May 2010.

[34] G. J. M. De Lannoy *et al.*, 'Converting Between SMOS and SMAP Level-1 Brightness Temperature Observations Over Nonfrozen Land', *IEEE Geosci. Remote Sensing Lett.*, vol. 12, no. 9, pp. 1908-1912, Sep. 2015.

[35] D. Entekhabi *et al.*, 'The Soil Moisture Active Passive (SMAP) Mission', *Proceedings of the IEEE*, vol. 98, no. 5, pp. 704-716, May 2010.

[36] J. R. Piepmeier *et al.*, 'SMAP L-Band Microwave Radiometer: Instrument Design and First Year on Orbit', *IEEE Transactions on Geoscience and Remote Sensing*, vol. 55, no. 4, pp. 1954-1966, Apr. 2017.

[37] L. Brocca, F. Melone, T. Moramarco, W. Wagner, and S. Hasenauer, 'ASCAT soil wetness index validation through in situ and modeled soil moisture data in central Italy', *Remote Sensing of Environment*, vol. 114, no. 11, pp. 2745-2755, Nov. 2010.

[38] I. E. Mladenova *et al.*, 'Remote monitoring of soil moisture using passive microwave-based techniques — Theoretical basis and overview of selected algorithms for AMSR-E', *Remote Sensing of Environment*, vol. 144, pp. 197-213, Mar. 2014.

[39] R. M. Parinussa, T. R. H. Holmes, N. Wanders, W. A. Dorigo, and R. A. M. de Jeu, 'A Preliminary Study toward Consistent Soil Moisture from AMSR2', *Journal of Hydrometeorology*, vol. 16, no. 2, pp. 932-947, Apr. 2015.

[40] D. P. Dee *et al.*, 'The ERA-Interim reanalysis: configuration and performance of the data assimilation system', *Quarterly Journal of the Royal Meteorological Society*, vol. 137, no. 656, pp. 553-597, 2011.

[41] R. Gelaro *et al.*, 'The Modern-Era Retrospective Analysis for Research and Applications, Version 2 (MERRA-2)', *J. Climate*, vol. 30, no. 14, pp. 5419-5454, Jul. 2017.

[42] S. Saha *et al.*, 'The NCEP Climate Forecast System Reanalysis', *Bulletin of the American Meteorological Society*, vol. 91, pp. 1015-1057, Aug. 2010.

[43] P. De Rosnay, M. Drusch, D. Vasiljevic, G. Balsamo, C. Albergel, and L. Isaksen, 'A simplified extended Kalman filter for the global operational soil moisture analysis at ECMWF', *Quarterly Journal*

of the Royal Meteorological Society, vol. 139, no. 674, pp. 1199-1213, 2013.

[44] C. Albergel *et al.*, 'Evaluation of remotely sensed and modelled soil moisture products using global ground-based in situ observations', *Remote Sensing of Environment*, vol. 118, pp. 215-226, Mar. 2012.

[45] G. Faye *et al.*, 'Soil moisture estimation in Ferlo region (Senegal) using radar (ENVISAT/ASAR) and optical (SPOT/VEGETATION) data', *The Egyptian Journal of Remote Sensing and Space Science*, vol. 21, pp. S13–S22, Jul. 2018.

[46] G. Faye, P. Louis Frison, S. Wade, J. Ndione, A. Chedikh Beye, and J. P. Rudant, 'ÉTUDE DE LA SAISONNALITÉ DES MESURES DES DIFFUSIOMÈTRES SCAT : APPORT AU SUIVI DE LA VÉGÉTATION AU SAHEL, CAS DU FERLO AU SÉNÉGAL', *Teledetection*, vol. 10, no. 1, pp. 23-31, Sep. 2011.

[47] J.-A. Ndione, J.-P. Lacaux, Y. Tourre, C. Vignolles, D. Fontanaz, and M. Lafaye, 'Mares temporaires et risques sanitaires au Ferlo : contribution de la télédétection pour l'étude de la fièvre de la vallée du Rift entre août 2003 et janvier 2004', *Science et Changements Planetaires - Secheresse*, vol. 20, Jan. 2009.

[48] S. Cissé, L. Eymard, C. Ottlé, J. A. Ndione, A. T. Gaye, and F. Pinsard, 'Rainfall Intra-Seasonal Variability and Vegetation Growth in the Ferlo Basin (Senegal)', *Remote Sensing*, vol. 8, no. 1, Art. no. 1, Jan. 2016.

[49] J.-A. Ndione, J.-P. Lacaux, Y. Tourre, C. Vignolles, D. Fontanaz, and M. Lafaye, 'Mares temporaires et risques sanitaires au Ferlo : contribution de la télédétection pour l'étude de la fièvre de la vallée du Rift entre août 2003 et janvier 2004', *Sécheresse*, vol. 20, no. 1, pp. 153-160, Jan. 2009.

[50] G. Kargas and P. Kerkides, 'Water content determination in mineral and organic porous media by ML2 theta probe', *Irrigation and Drainage*, vol. 57, no. 4, pp. 435-449, 2008.

[51] J.-P. Wigneron *et al.*, 'Modelling the passive microwave signature from land surfaces: A review of recent results and application to the L-band SMOS & SMAP soil moisture retrieval algorithms', *Remote Sensing of Environment*, vol. 192, pp. 238-262, Apr. 2017.

[52] S. K. Chan *et al.*, 'Development and assessment of the SMAP enhanced passive soil moisture product', *Remote Sensing of Environment*, vol. 204, pp. 931-941, Jan. 2018.

[53] A. J. Purdy *et al.*, 'SMAP soil moisture improves global evapotranspiration', *Remote Sensing of Environment*, vol. 219, pp. 1-14, Dec. 2018.

[54] D. Entekhabi *et al.*, 'SMAP Handbook–Soil Moisture Active Passive: Mapping Soil Moisture and Freeze/Thaw from Space', Jan. 2014, Accessed: Feb. 24, 2021. [Online]. Available: https://lirias.kuleuven.be/1741023.

[55] ONeill, Peggy E., Chan, Steven, Njoku, Eni G., Jackson, Tom, Bindlish, Rajat, and Chaubell, M. Julian, 'SMAP L3 Radiometer Global Daily 36 km EASE-Grid Soil Moisture, Version 7'. NASA National Snow and Ice Data Center DAAC, 2020.

[56] J. D. Bolten and W. T. Crow, 'Improved prediction of quasi-global vegetation conditions using remotely-sensed surface soil moisture', *Geophysical Research Letters*, vol. 39, no. 19, 2012.

[57] ONeill, Peggy E., Chan, Steven, Njoku, Eni G., Jackson, Tom, and Bindlish, Rajat, 'SMAP L3 Radiometer Global Daily 36 km EASE-Grid Soil Moisture, Version 6'. NASA National Snow and Ice Data Center DAAC, 2019.

[58] R. H. Reichle *et al.*, 'Global Assessment of the SMAP Level-4 Surface and Root-Zone Soil Moisture Product Using Assimilation Diagnostics', *Journal of Hydrometeorology*, vol. 18, no. 12, pp. 3217-3237, Dec. 2017.

[59] R. H. Reichle *et al.*, 'Assessment of the SMAP Level-4 Surface and Root-Zone Soil Moisture Product Using In Situ Measurements', *Journal of Hydrometeorology*, vol. 18, no. 10, pp. 2621-2645, Oct. 2017.

[60] S. Swain, B. D. Wardlow, S. Narumalani, D. C. Rundquist, and M. J. Hayes, 'Relationships between vegetation indices and root zone soil moisture under maize and soybean canopies in the US Corn Belt: a comparative study using a close-range sensing approach', *International Journal of Remote Sensing*, vol. 34, no. 8, pp. 2814-2828, Apr. 2013.

[61] A. Al Bitar *et al.*, 'Evaluation of SMOS Soil Moisture Products Over Continental U.S. Using the SCAN/SNO ^{TEL} Network', *IEEE Transactions on Geoscience and Remote Sensing*, vol. 50, no. 5, pp. 1572-1586, May 2012.

[62] Y. H. Kerr *et al.*, 'The SMOS Mission: New Tool for Monitoring Key Elements ofthe Global Water Cycle', *Proceedings of the IEEE*, vol. 98, no. 5, pp. 666-687, May 2010.

[63] T. J. Jackson *et al.*, 'Validation of Soil Moisture and Ocean Salinity (SMOS) Soil Moisture Over Watershed Networks in the U.S.', *IEEE Transactions on Geoscience and Remote Sensing*, vol. 50, no. 5, pp. 1530-1543, May 2012.

[64] O. Merlin, C. Rudiger, A. A. Bitar, P. Richaume, J. P. Walker, and Y. H. Kerr, 'Disaggregation of SMOS Soil Moisture in Southeastern Australia', *IEEE Transactions on Geoscience and Remote Sensing*, vol. 50, no. 5, pp. 1556-1571, May 2012.

[65] O. Merlin, Y. Malbéteau, Y. Notfi, S. Bacon, S. Khabba, and L. Jarlan, 'Performance Metrics for Soil Moisture Downscaling Methods: Application to DISPATCH Data in Central Morocco', *Remote Sensing*, vol. 7, no. 4, pp. 3783-3807, Mar. 2015.

[66] A. A. Bitar, Y. Kerr, O. Merlin, F. Cabot, and J.-P. Wigneron, 'Root zone soil moisture and drought index from SMOS', p. 2.

[67] C. Funk *et al.*, 'The climate hazards infrared precipitation with stations—a new environmental record for monitoring extremes', *Sci Data*, vol. 2, no. 1, p. 150066, Dec. 2015.

[68] T. Dinku *et al.*, 'Validation of the CHIRPS satellite rainfall estimates over eastern Africa', *Quarterly Journal of the Royal Meteorological Society*, vol. 144, no. S1, pp. 292-312, 2018.

[69] C. Funk *et al.*, 'The collaborative historical African rainfall model: description and evaluation', *International Journal of Climatology*, vol. 23, no. 1, pp. 47-66, 2003.

[70] C. Albergel *et al.*, 'A first assessment of the SMOS data in southwestern France using in situ and airborne soil moisture estimates: The CAROLS airborne campaign', *Remote Sensing of Environment*, vol. 115, no. 10, pp. 2718-2728, Oct. 2011.

[71] T. J. Jackson *et al.*, 'Validation of Advanced Microwave Scanning Radiometer Soil Moisture Products', *IEEE Transactions on Geoscience and Remote Sensing*, vol. 48, no. 12, pp. 4256-4272, Dec. 2010.

[72] T. J. Jackson *et al.*, 'Validation of Soil Moisture and Ocean Salinity (SMOS) Soil Moisture Over Watershed Networks in the U.S.', *IEEE Transactions on Geoscience and Remote Sensing*, vol. 50, no. 5, pp. 1530-1543, May 2012.

[73] F. Lei, W. T. Crow, H. Shen, R. M. Parinussa, and T. R. H. Holmes, 'The Impact of Local Acquisition Time on the Accuracy of Microwave Surface Soil Moisture Retrievals over the Contiguous United States', *Remote Sensing*, vol. 7, no. 10, Art. no. 10, Oct. 2015.

[74] A. Al-Yaari *et al.*, 'Evaluating soil moisture retrievals from ESA's SMOS and NASA's SMAP brightness temperature datasets', *Remote Sensing of Environment*, vol. 193, pp. 257-273, May 2017.

[75] X. Li *et al.*, 'Compared performances of SMOS-IC soil moisture and vegetation optical depth retrievals based on Tau-Omega and Two-Stream microwave emission models', *Remote Sensing of Environment*, vol. 236, p. 111502, Jan. 2020.

[76] C. Gruhier and G. Quantin, 'SMOS soil moisture product evaluation over West-Africa from local to regional scale', *Remote Sensing of Environment*, Accessed: Jul. 07, 2021. [Online]. Available: https://www.academia.edu/23265522/SMOS_soil_moisture_product_evaluation_over_West_Africa_from_local_to_regional_scale.

[77] Z. Liu, P. Li, and J. Yang, 'Soil Moisture Retrieval and Spatiotemporal Pattern Analysis Using Sentinel-1 Data of Dahra, Senegal', *Remote Sensing*, vol. 9, no. 11, Art. no. 11, Nov. 2017.

[78] C. Gruhier *et al.*, 'Soil moisture active and passive microwave products: intercomparison and evaluation over a Sahelian site', *Hydrology and Earth System Sciences*, vol. 14, no. 1, pp. 141-156, 2010.

[79] F. Baup *et al.*, 'Mapping surface soil moisture over the Gourma mesoscale site (Mali) by using ENVISAT ASAR data', *Hydrology and Earth System Sciences*, vol. 15, no. 2, pp. 603-616, Feb. 2011.

[80] H. Vereecken *et al.*, 'On the spatio-temporal dynamics of soil moisture at the field scale', *Journal of Hydrology*, vol. 516, pp. 76-96, Aug. 2014.